

An n-Si/n-Fe₂O₃ Heterojunction Tandem Photoanode for Solar Water Splitting

Roel van de Krol^{*ab} and Yongqi Liang^b

Abstract: Few metal oxide photoanodes are able to reduce protons to hydrogen because their conduction band minimum is located at too positive potentials. This can be remedied by biasing the photoanode with a photovoltaic cell placed behind the photoanode. The disadvantage of such a tandem device is the rather complicated structure. Here, we demonstrate a very simple monolithic heterojunction tandem photoanode based on n-Si and n-type α -Fe₂O₃. Detailed characterization of this system in a basic planar configuration reveals that the silicon generates a photovoltage of ~ 0.3 V, and that the heterojunction functions as a D4 tandem device in which the absorption of two photons leads to one high-energy electron in the external circuit. No Fermi level pinning occurs at the Si/Fe₂O₃ interface, and the tandem photoanode is thermodynamically able to split water without the need for an external bias potential. This suggests that the n-Si/n-Fe₂O₃ heterojunction photoanode is a promising system for solar water splitting.

Keywords: Hematite · Heterojunction · Silicon · Tandem photoanode · Water splitting

1. Introduction

The hematite form of iron oxide, α -Fe₂O₃, is a promising material for solar water splitting. It is highly stable in alkaline solutions, and with a bandgap of 2.1 eV its maximum theoretical solar-to-hydrogen conversion efficiency is 15.3%. Recent breakthroughs, mainly by Grätzel and co-workers at EPFL, in the synthesis of highly porous, cauliflower-like nanostructures,^[1] interfacial (under)layers,^[2,3] and water oxidation co-catalysts^[4,5] have resulted in photocurrents above 3 mA/cm² under AM1.5G illumination.^[6]

Two important challenges for this material remain. The first is to further optimize the morphology of the electrode to combat the small minority carrier diffusion length in this material (2–4 nm^[7]). Nanowire arrays,^[8,9] porous colloidal systems^[10] as well as host absorber–guest scaffold structures^[11] have been explored, but their performance has not yet reached the level of the cauliflower-based structures made by atmospheric pressure chemical vapor deposition (APCVD).

The second challenge is to ‘boost’ the energy of the photo-generated electrons

with a bias voltage to enable the reduction of water to H₂. This is necessary because the conduction band of Fe₂O₃ is located at ~ 0.2 – 0.3 eV below the H₂/H⁺ redox energy.^[2,12] Since hematite only absorbs light with wavelengths below 590 nm, the bias voltage can be generated by placing a second absorber or photovoltaic device behind the hematite film. Solar-to-hydrogen efficiencies of 1.17% have recently been reported for an APCVD-hematite photoanode biased with a dye sensitized solar cell (DSC) in a so-called D4 configuration (dual absorber, four photons per H₂).^[13]^[14] This is still much lower than the 15.3% theoretical efficiency for three main reasons: the high photocurrent onset potential (*i.e.* poor water oxidation catalysis) of the hematite combined with the modest voltage of the DSC,^[14] light scattering in the nanostructured hematite which prevents part of the light from reaching the DSC,^[15] and the relatively low quantum efficiencies of the hematite photoanodes.^[4]

In this paper we explore a so-called n–n

heterojunction as an alternative method to boost the energy of the photogenerated electrons in hematite. The heterojunction consists of a thin hematite film that is deposited directly onto an n-type silicon wafer. The simple planar structure ensures that the analysis of this structure is relatively straightforward, *i.e.* without the complications due to light scattering or non-trivial potential distributions that one encounters in mesoporous nanostructured systems. We will show that the silicon is able to generate a photovoltage of ~ 0.3 V, and that this is in principle sufficient to split water without the need for an external bias potential.

2. Device Concept

The principle of the Si/Fe₂O₃ heterojunction photoanode is illustrated in Fig. 1. The n-type Fe₂O₃ forms a semiconductor/liquid junction with the aqueous electrolyte and absorbs the blue/green photons.

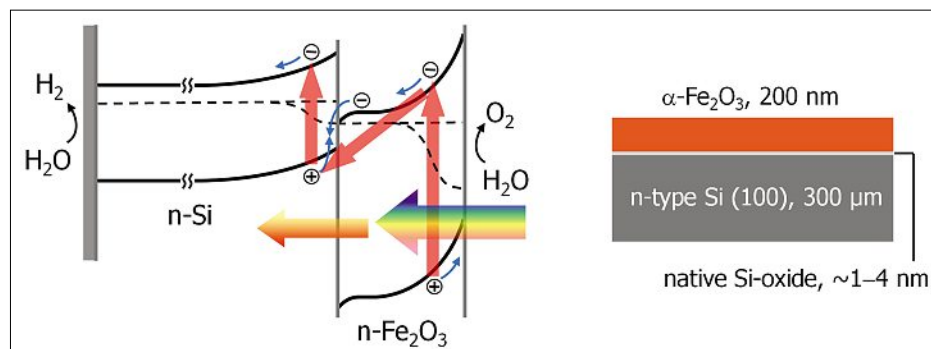


Fig. 1. Band diagram of an n-Si/n-Fe₂O₃ heterojunction tandem photoanode (left), and the planar implementation of the heterojunction studied in this paper (right).

*Correspondence: Dr. R. van de Krol^{ab}

Tel.: +49 30 8062 43035

E-mail: roel.vandekrol@helmholtz-berlin.de

^aHelmholtz-Zentrum Berlin für Materialien und Energie GmbH

Hahn-Meitner-Platz 1

D-14109 Berlin, Germany

^bDelft University of Technology

Department of Chemical Engineering

Materials for Energy Conversion and Storage (MECS)

P.O. Box 5045, 2600 GA Delft, The Netherlands

The red photons are transmitted and subsequently absorbed in the n-type silicon. Since silicon has a lower work function than hematite (*vide infra*), an n–n heterojunction is formed at the Si/hematite interface and the resulting field in the silicon separates the electrons and holes. The photogenerated holes in the silicon recombine with the photo-generated electrons in the Fe_2O_3 at the interface. The diagram in Fig. 1 clearly shows that this is also a D4-type configuration; in fact, it is the simplest form of a D4 device for solar water splitting that one can imagine. The system works in a way that is similar to the Z-scheme formed by photosystems I and II in the natural photosynthesis process.

It should be noted that a thin native SiO_x layer between the silicon and the hematite is always present. In our case this is unavoidable since the hematite is deposited by spray deposition at elevated temperature in ambient air. Hence, no efforts are made to remove the native oxide. Presumably, electron-hole recombination at the Si/ Fe_2O_3 interface will take place within this layer.

3. Experimental

Thin films of undoped Fe_2O_3 were deposited onto n-type Si substrates (phosphorus-doped, 10–20 $\Omega\cdot\text{cm}$, (100)-orientation) by spray pyrolysis of a solution of 0.04 M $\text{Fe}(\text{AcAc})_3$ in a mixed solvent of ethyl acetate and ethanol (2:1). The deposition was carried out using a glass pneumatic atomizer (CAMAG, 022.6100) with compressed air as a carrier gas. To avoid large fluctuations of the temperature during spraying and to give the solvent enough time to evaporate, the deposition was carried out using a 15 s on – 45 s off cycle. The substrate temperature was 400 $^\circ\text{C}$; at this temperature, further thermal growth of the Si native oxide layer is negligible. Control samples of $\alpha\text{-Fe}_2\text{O}_3$ were deposited on conducting glass (FTO, TEC15, Libbey-Owens-Ford).^[16]

Photoelectrochemical measurements were carried out in a three-electrode cell made of Teflon, with a fused silica window through which the sample can be illuminated.^[17] A 1.0 M KOH aqueous solution (pH 13.6) was used as the electrolyte. A Ga–In eutectic alloy was used to form an Ohmic back-contact to the silicon. The potential of the working electrode (\varnothing 6 mm, 0.283 cm^2) was controlled by an EG&G 283 potentiostat (Princeton Applied Research). An Ag/AgCl electrode (REF321, Radiometer Analytical) and a coiled Pt wire were used as the reference and counter electrodes, respectively. In the rest of the paper, all potentials are converted to the reversible hydrogen scale (RHE).^[17]

The I–V curves were measured at a scan rate of 20 mV/s, or 4 mV/s if chopped illumination was used. An array of 19 LEDs (375 nm, Roithner Lasertechnik) was used as a UV light source, and focussing onto the sample with a quartz lens gave an intensity of ~ 1 mW/cm^2 . Red light illumination was provided by a 635 nm diode laser module (5 mW, Coherent), attenuated by metal-film neutral density filters (Melles Griot) to give intensities between 100 nW/cm^2 and 10 mW/cm^2 .

4. Results and Discussion

To investigate the basic characteristics of the Si/ Fe_2O_3 junction, current–voltage measurements have first been carried out in the dark (Fig. 2A). At negative applied potentials, the onset for cathodic currents is shifted to ~ 0.13 V more negative values compared to the FTO/ Fe_2O_3 control sample (ΔV in Fig. 2A). This is largely due to the built-in voltage, V_{bi} , at the Si/hematite junction (Fig. 2B) which has to be overcome before current can start flowing in the forward direction (Fig. 2C). Under reverse bias conditions, (dark) electrochemical oxidation of water starts at ~ 1.7 V for the FTO/ Fe_2O_3 control sample. For the Si/ Fe_2O_3 sample, no anodic currents are observed since most of the potential drop falls across the silicon (Fig. 2D).

The fact that most of the applied potential falls across the silicon space charge region is due to its much smaller donor density ($\sim 3 \times 10^{14} \text{ cm}^{-3}$) compared to that of the Fe_2O_3 ($\sim 2 \times 10^{17} \text{ cm}^{-3}$).^[2] One can also think of the system as two capacitances in series, so that the distribution of any change in the externally applied potential can be written as $\Delta V_{\text{SC,Si}}/\Delta V_{\text{SC, hematite}} = C_{\text{SC, hematite}}/C_{\text{SC,Si}}$. Assuming a dielectric constant of 11.9 and a potential drop of 0.3 V within the silicon space charge under equilibrium conditions (*vide infra*), the corresponding space charge capacitance, $C_{\text{SC,Si}}$, is ~ 9.6 nF/cm^2 . The equilibrium potential drop within the $\alpha\text{-Fe}_2\text{O}_3$ space charge can be estimated from the difference between the pH (13.6) and its point of zero charge (pzc), which is 8.5.^[18] This gives an upward band bending of $(13.6 - 8.5) \times 59 \text{ mV/pH} = 0.30$ V under open circuit conditions. Assuming a dielectric constant of 80,^[12] this results in a space charge capacitance ($C_{\text{SC,Si}}$) of ~ 0.64 $\mu\text{F}/\text{cm}^2$ for the hematite film. The fraction of ΔV_{total} that falls across the Si is given by $\Delta V_{\text{SC,Si}}/(\Delta V_{\text{SC,Si}} + \Delta V_{\text{SC, hematite}}) = 640/(640 + 9.6) = 0.985$. Hence, more than 98% of any change in the externally applied potential will fall across the silicon space charge.

To obtain a more accurate value of the band bending within the silicon at the Si/ Fe_2O_3 interface, the open circuit potential (OCP) was measured as a function of the

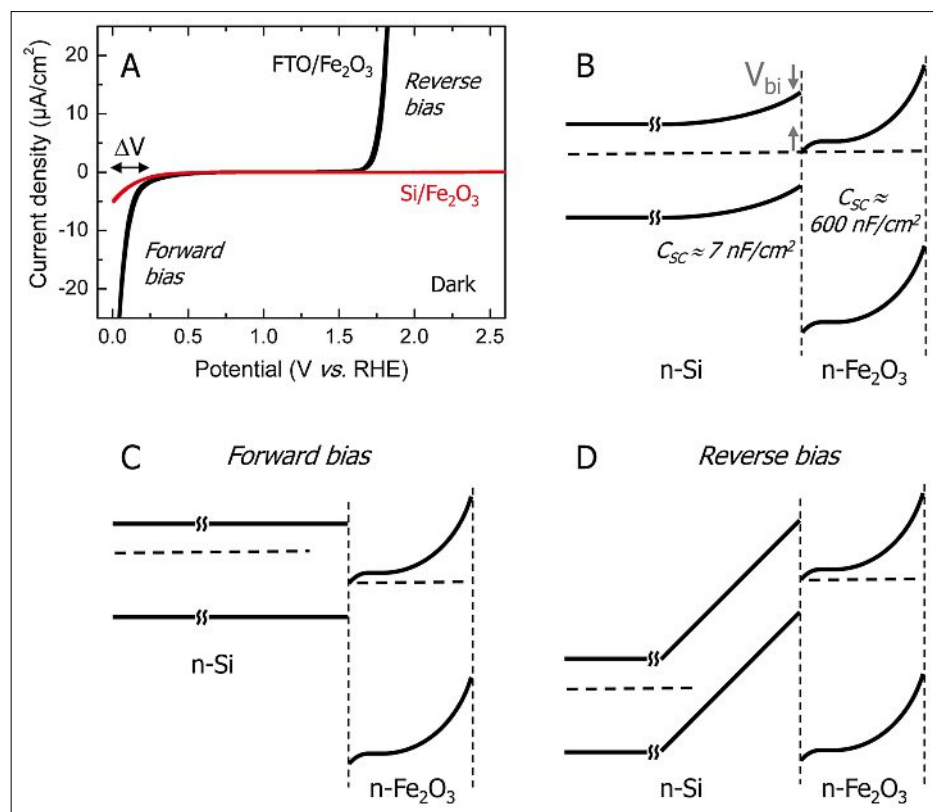


Fig. 2. (A) Dark voltammograms of a 200 nm Fe_2O_3 film deposited on FTO (black curve) and on n-type silicon (red curve). (B) Band diagram of the n-Si/n- Fe_2O_3 heterojunction under equilibrium conditions in the dark. (C) Band diagram of the heterojunction in the dark under forward and (D) reverse bias.

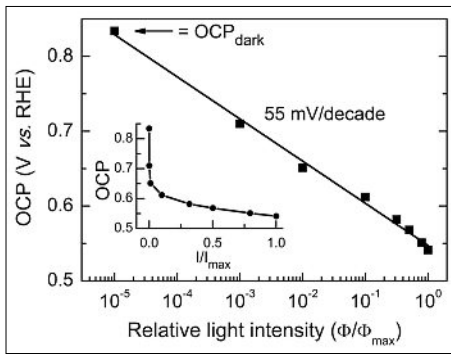


Fig. 3. Open circuit potential (OCP) as a function of light intensity for the n-Si/n-Fe₂O₃ heterojunction under illumination with 635 nm light. Only the Si is excited, absorption in the α-Fe₂O₃ is negligible. The inset shows the same data on a linear scale, indicating the OCP is close to its saturation value at the highest light intensities.

incident light intensity (Fig. 3). A wavelength of 635 nm (1.95 eV) was used to ensure that only the silicon is excited; no absorption occurs in the Fe₂O₃ due to its larger bandgap (2.1 eV). The OCP is close to saturation at the highest light intensities (inset Fig. 3), and is 0.30 V more negative than the value in the dark. This proves the presence of a photoactive junction in the silicon and shows that the maximum band bending in the silicon is ~0.30 V.

Another interesting observation from Fig. 3 is that the slope of the curve corresponds to an OCP change of 55 mV per decade change in light intensity. This is close to the theoretically expected value of 59 mV that follows from Eqn. (1) given by Rajeshwar for a single junction under illumination:^[19]

$$V_{oc} = \frac{kT}{e} \ln \left(\frac{i_{ph}}{i_0} \right) \quad (1)$$

Here, i_{ph} is the photocurrent density due to the minority carriers (which is assumed to be proportional to the light intensity), and i_0 is the exchange current density under equilibrium conditions in the dark. The small difference between the observed and the theoretical value of the slope implies that there is no Fermi level pinning at the interface. So despite the presence of the native oxide layer, the Si/SiO_x/Fe₂O₃ interface behaves in a nearly ideal fashion.

In an earlier study on spray-deposited hematite photoanodes made with the same spray recipe, we reported a flatband potential of +0.17 V vs RHE.^[2] This corresponds to an energy of ~4.7 eV below the vacuum level. For n-type silicon with a donor density (N_D) of $\sim 3 \times 10^{14} \text{ cm}^{-3}$, the work function is given by $\chi_A + (E_C - E_F) = 4.05 + kT \ln(N_C/N_D) \approx 4.36 \text{ eV}$ (χ_A is the electron affinity and N_C is the effective density of states in the conduction band of Si).^[20] This gives a

value of ~0.3 V for the difference between the Si and Fe₂O₃ work functions, which matches very well with the value found for the maximum band bending in the Si/Fe₂O₃ heterojunction.

Fig. 4 shows the photocurrent as a function of applied potential under chopped illumination with the same 635 nm light source. Only transient current spikes are observed, the steady-state photocurrent is negligible. This is consistent with the proposed band diagram, shown again in the inset of Fig. 4. The photo-generated electrons in the silicon are driven to the back-contact by the built-in electric field, which causes the positive transient response. Transport of the holes, however, is blocked by the large valence band offset between the silicon and the hematite. The holes therefore recombine with conduction band electrons, which explains the negative current transients. Together with the data from Fig. 2A and Fig. 3, this conclusively proves the presence of a n-n heterojunction at the Si/Fe₂O₃ interface.

Voltammograms for the n-Si/n-Fe₂O₃ heterojunction under continuous illumination are shown in Fig. 5. The currents are negligible in the dark and under 635 nm excitation, consistent with the results dis-

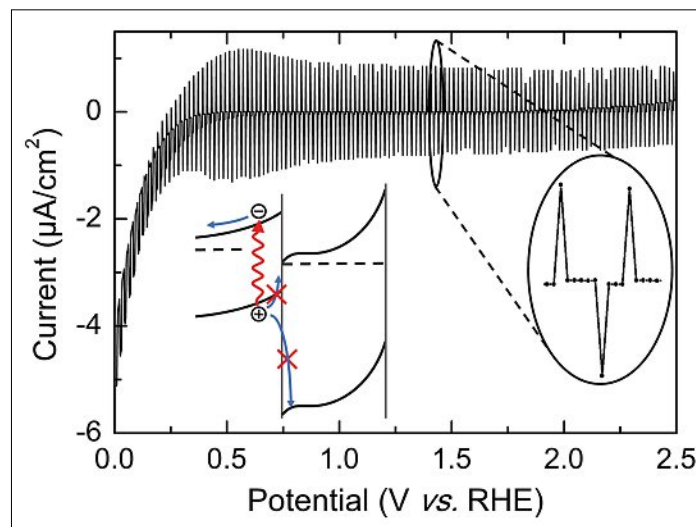


Fig. 4. Chopped-light voltammograms of a n-Si/n-Fe₂O₃ heterojunction under 635 nm illumination. The inset on the right shows a magnification of the current transients. The bottom-left inset shows the band diagram that explains the transient response.

cussed above. When exciting the Fe₂O₃ with 375 nm light, a modest anodic photocurrent is observed (blue curve with $\Phi_{635}/\Phi_{375} = 0$). Under these conditions only the Fe₂O₃ is excited, and the photo-generated electrons are conducted to the back-contact via the silicon. When illuminating with both 375 and 635 nm light, the photocurrent is much larger than the sum of the individual 375 nm and 635 nm photocurrents. Moreover, an ~0.3 V cathodic shift of the photocurrent onset potential is observed when compared to the 375 nm curve. These observations prove that the Si/Fe₂O₃ heterojunction indeed functions as a two-photon tandem device.

It is somewhat surprising that excitation with only 375 nm light gives a measurable photocurrent; according to the band diagram in Fig. 1, photo-excited electrons in Fe₂O₃ should not be able to reach the back contact unless the silicon is also excited. With an Fe₂O₃ absorption coefficient of $3.5 \times 10^5 \text{ cm}^{-1}$ at 375 nm,^[21] only 0.09% of the incident photons will reach the silicon by transmission through the 200 nm Fe₂O₃ film. The highest photocurrent that one could expect from these transmitted photons is $0.27 \mu\text{A}/\text{cm}^2$ for the light intensity used ($1 \text{ mW}/\text{cm}^2$), assuming 100% quantum efficiency in the silicon. Hence, excitation of Si by un-absorbed 375 nm photons cannot explain the much larger current densities observed in Fig. 5. Instead, we tentatively attribute the photocurrent to thermal generation of carriers under strong depletion conditions. The photocurrent starts to increase at potentials >1.1 V vs. RHE. With an OCP of 0.83 V_{RHE} (in the dark) and a built-in potential of 0.3 V, the total potential across the space charge region amounts to ~0.6 V, *i.e.* more than half the bandgap of silicon (1.12 eV). This will strongly increase the concentration of thermally generated holes in the valence band of the silicon, and may even

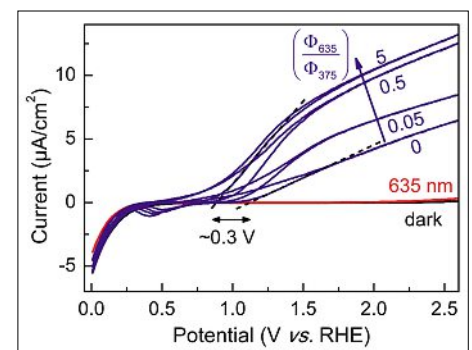


Fig. 5. Voltammograms of an n-Si/n-Fe₂O₃ heterojunction in the dark and under illumination with 635 nm, 375 nm, and 375 nm + 635 nm light.

lead to the formation of an inversion layer. These holes can recombine with the photo-generated electrons in the Fe_2O_3 , thus closing the current circuit.

Further evidence for the two-photon tandem mode of operation is given by the chopped-light voltammograms shown in Fig. 6. Under 375 nm illumination, a sign reversal of the photocurrent occurs at $\sim 0.12 \text{ V}_{\text{RHE}}$. This is close to the open circuit potential in the dark ($0.83 \text{ V}_{\text{RHE}}$) minus the built-in potentials of the Si and the Fe_2O_3 (both 0.30 V , *vide supra*). In other words, close to the potential where both the Si and the Fe_2O_3 bands are expected to flatten out. Upon co-illumination with 635 nm light, the transition potential shifts cathodically by at least 0.3 V as shown in the right-hand side of Fig. 6. The observation of anodic photocurrents at a potential that is negative of the hydrogen evolution potential shows that the Si is indeed able to boost the energy of the electrons above the H_2/H^+ energy level. Moreover, since the Fe_2O_3 valence band is located at a potential more positive than the oxygen evolution potential,^[22] we can conclude that water splitting is thermodynamically possible with a n-Si/n- Fe_2O_3 heterojunction photoanode.

5. Conclusions

We have demonstrated a composite photoanode based on a simple n-n heterojunction of silicon and $\alpha\text{-Fe}_2\text{O}_3$. Detailed characterization of this system shows that the silicon generates a photovoltage of $\sim 0.3 \text{ V}$, and that the heterojunction functions as a tandem device in which the absorption of two photons leads to one high-energy electron in the external circuit. As a result, the tandem photoanode is thermodynamically able to split water without the need for an external bias potential. The efficiency of this un-optimized tandem photoanode is presumably limited by extensive recombination in the Fe_2O_3 as

well as Ohmic losses due to the presence of a native SiO_x layer at the Si/ Fe_2O_3 interface. Exploration of nanowire array architectures and reduction of the native oxide thickness are promising avenues to address these issues. In fact, during the preparation of this work the group of Wang *et al.* published an interesting paper demonstrating AM1.5 photocurrents slightly above 0.6 mA/cm^2 at 1.0 V vs. RHE for a Si nanowire array coated with a thin $\alpha\text{-Fe}_2\text{O}_3$ film.^[23] After optimizing the materials and their interfaces, accurate current matching of the Fe_2O_3 and Si junctions would be the next step. The excellent photochemical stability of Fe_2O_3 ensures that the silicon is well protected against photocorrosion. In view of the nearly ideal behavior of the Si/ SiO_x / Fe_2O_3 interface (no Fermi level pinning) and the simple configuration of this D4 system, the silicon/hematite appears to be a promising materials combination that may offer exciting possibilities for economically feasible solar water splitting.

Acknowledgements

This work is financially supported by the Sustainable Hydrogen program (project nr. 053.61.009) of NWO-ACTS. The authors thank Prof. Bernard Dam for stimulating discussions.

Received: January 9, 2013

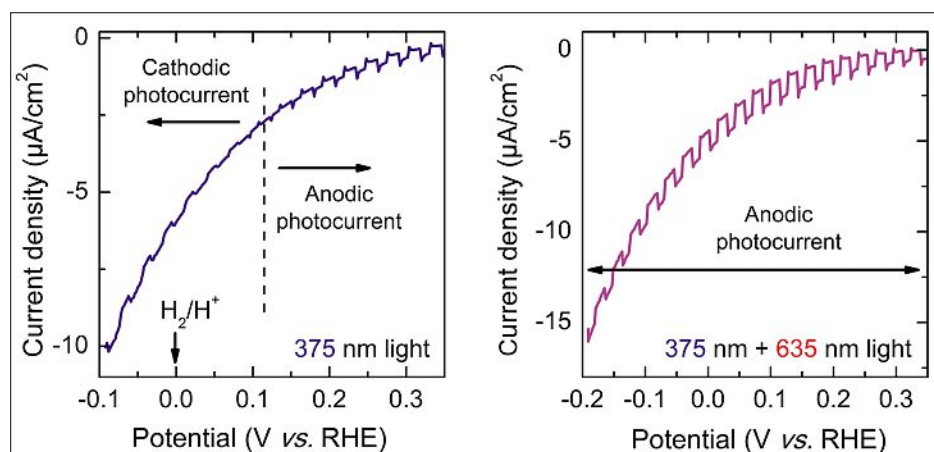


Fig. 6. Chopped-light voltammograms of an n-Si/n- Fe_2O_3 heterojunction under 375 nm illumination (left) and under 375 nm + 635 nm illumination (right).

- J. B. Jasinski, V. Kumar, T. Deutsch, M. K. Sunkara, *Nanotechnol.* **2012**, *23*, 194009.
- [10] J. Brilliet, M. Grätzel, K. Sivula, *Nano Lett.* **2010**, *10*, 4155.
- [11] K. Sivula, F. Le Formal, M. Grätzel, *Chem. Mater.* **2009**, *21*, 2862.
- [12] J. H. Kennedy, K. W. Frese, Jr., *J. Electrochem. Soc.* **1978**, *125*, 723.
- [13] J. R. Bolton, S. J. Strickler, J. S. Connolly, *Nature* **1985**, *316*, 495.
- [14] J. Brilliet, J. H. Yum, M. Cornuz, T. Hisatomi, R. Solarzka, J. Augustynski, M. Grätzel, K. Sivula, *Nature Photon.* **2012**, *6*, 823.
- [15] J. Brilliet, M. Cornuz, F. Le Formal, J. H. Yum, M. Grätzel, K. Sivula, *J. Mater. Res.* **2010**, *25*, 17.
- [16] Y. Q. Liang, R. van de Krol, *Chem. Phys. Lett.* **2009**, *479*, 86.
- [17] 'Photoelectrochemical Hydrogen Production', Eds. R. van de Krol, M. Grätzel, Springer, New York, **2012**.
- [18] N. Kallay, T. Preocanin, *J. Colloid Interf. Sci.* **2008**, *318*, 290.
- [19] K. Rajeshwar, in 'Encyclopedia of Electrochemistry, Volume 6: Semiconductor Electrodes and Photoelectrochemistry', Ed. S. Licht, Wiley, **2007**, p. 1.
- [20] S. M. Sze, 'Physics of Semiconductor Devices', John Wiley & Sons, New York, **1981**.
- [21] L. A. Marusak, R. Messier, W. B. White, *J. Phys. Chem. Solids* **1980**, *41*, 981.
- [22] R. van de Krol, Y. Q. Liang, J. Schoonman, *J. Mater. Chem.* **2008**, *18*, 2311.
- [23] M. T. Mayer, C. Du, D. W. Wang, *J. Am. Chem. Soc.* **2012**, *134*, 12406.

- [1] I. Cesar, A. Kay, J. A. G. Martinez, M. Grätzel, *J. Am. Chem. Soc.* **2006**, *128*, 4582.
- [2] Y. Q. Liang, C. S. Enache, R. van de Krol, *Int. J. Photoenergy* **2008**, 739864.
- [3] T. Hisatomi, H. Dotan, M. Stefik, K. Sivula, A. Rothschild, M. Grätzel, N. Mathews, *Adv. Mater.* **2012**, *24*, 2699.
- [4] S. D. Tilley, M. Cornuz, K. Sivula, M. Grätzel, *Angew. Chem. Int. Ed.* **2010**, *49*, 6405.
- [5] A. Kay, I. Cesar, M. Grätzel, *J. Am. Chem. Soc.* **2006**, *128*, 15714.
- [6] K. Sivula, F. Le Formal, M. Grätzel, *ChemSusChem* **2011**, *4*, 432.
- [7] J. H. Kennedy, K. W. Frese, Jr., *J. Electrochem. Soc.* **1978**, *125*, 709.
- [8] D. D. Qin, C. L. Tao, S. I. In, Z. Y. Yang, T. E. Mallouk, N. Z. Bao, C. A. Grimes, *Energy & Fuels* **2011**, *25*, 5257.
- [9] B. D. Chernomordik, H. B. Russell, U. Cvelbar,